

Predictive Model of Restart-Up Pressure Drop after Shutdown for Heavy Oil–Water Ring Transportation Pipeline

Xiaoyun Yin,* Ming Wen, Dong Lin, Jiayi Li, Zhen Zhu, Yu Zhang, Jinyan Hu, Pengsheng Zeng, Jiaqiang Jing,* and Jie Sun



Cite This: *ACS Omega* 2024, 9, 15439–15448

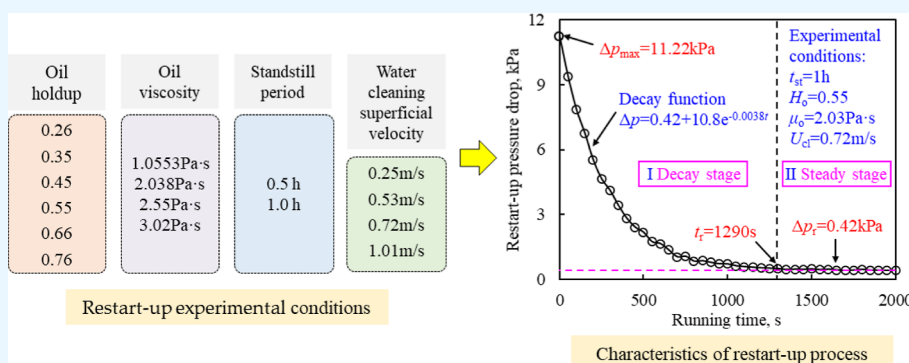


Read Online

ACCESS |

Metrics & More

Article Recommendations



ABSTRACT: Aiming at the problem of restart-up for a heavy oil–water ring transportation pipeline due to instability and damage of the water ring, based on the self-developed design of a small indoor loop simulation experimental device and taking four kinds of ordinary heavy oil in the Lvda oilfield as the research object, the change trend of restart-up pressure drop with time is experimentally studied when the pipeline is restarted-up after shutdown at a constant water flow. On the basis of the regression analysis of the orthogonal restart-up experimental data of four factors (oil holdup, oil viscosity, standstill period, and water cleaning superficial velocity) and mixed levels by the statistical product and service solutions statistical analysis software, a multivariate nonlinear restart-up maximum pressure drop prediction model is established. Through analysis of the characteristics of each stage of the restart-up process, an exponential decay model of restart-up pressure drop with time is created. The research results show that the variations in restart-up pressure drop with time can be divided into two stages: the attenuation stage and the equilibrium stage. The predicted value of restart-up pressure drop with time is in good agreement with the measured one, and the goodness of fit is very close to 1. The maximum restart-up pressure drop rises along with the increase in oil holdup, oil viscosity, standstill period, and water cleaning superficial velocity. The restart-up time prolongs with the increase in oil holdup, oil viscosity, and standstill period but shortens with the increase in water cleaning superficial velocity.

1. INTRODUCTION

With the continuous growth of the crude oil demand and the increasing scarcity of conventional crude oil, the supply of crude oil resources in the world is shifting from light oil to heavy oil. The abundant reserves of heavy oil is bound to play an important role in the global energy market in the coming decades.^{1–5} However, due to its high viscosity, high density, and poor fluidity, heavy oil poses great difficulties and challenges in its extraction, storage, and processing.⁶ At present, pipeline transportation of heavy oil is mainly achieved through three ways: first, viscosity reduction, which refers to reducing the viscosity of crude oil. Possible measures include heating (preheating heavy oil or heating pipelines),⁷ dilution (adding diluent with lower viscosity than the heavy oil),⁸ emulsification (adding surfactant to heavy oil to form oil-in-water emulsion),⁹ etc.; second, drag reduction, which refers to reducing the

frictional resistance between heavy oil and the pipe wall. Possible methods include adding drag reducer¹⁰ and forming an annular flow structure with a low viscosity liquid ring surrounding a high viscosity oil core;¹¹ third, oil upgrading,¹² which refers to modifying heavy oil on-site to produce synthetic crude oil with lower viscosity, higher API degree, lower asphaltene, heavy metal, and sulfur content. Among them, the low-viscosity liquid ring method, especially the water ring transportation method,

Received: January 6, 2024

Revised: February 14, 2024

Accepted: February 22, 2024

Published: March 20, 2024



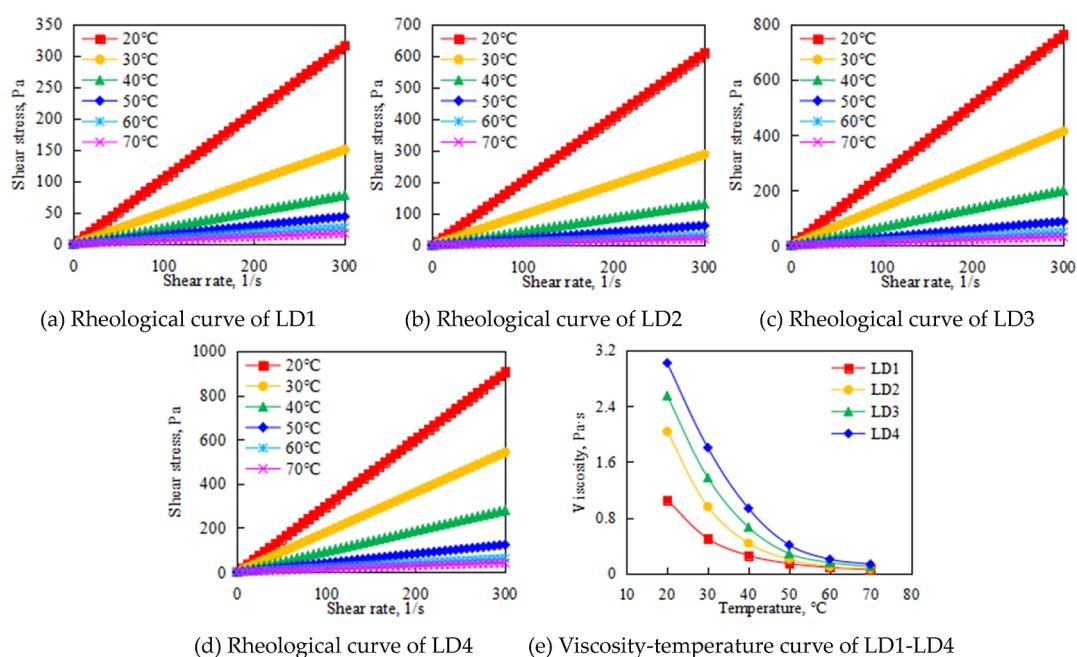


Figure 1. Rheological properties and viscosity–temperature characteristics of Lvda heavy oils.

has attracted widespread attention from scholars in related fields worldwide due to its significant advantages of low energy consumption and environmental friendliness. It is regarded as one of the most promising heavy oil transportation methods for industrial applications.¹³

In recent years, scholars at home and abroad have conducted a large amount of theoretical analysis, experimental research, and numerical simulation on the heavy oil–water ring transportation technology, where they have mainly focused on the problems of heavy oil–water ring transportation under normal operating conditions, such as the optimization design of water ring generators and their auxiliary components,^{14–16} the lubrication and drag reduction mechanism of heavy oil–water ring transportation,^{17–19} the flow pattern and pressure drop characteristics of heavy oil–water ring flow,^{20–23} and the enhancement measures for the flow stability of heavy oil–water ring flow.^{24–27} However, little attention has been paid to the difficult problem of restarting after shutdown due to planned maintenance or unexpected shutdown. In view of this, four ordinary heavy oils from the Lvda oilfield and tap water are taken as research objects, and a simulation experimental system is independently designed and developed to investigate the flow, shutdown, and restart-up of the heavy oil–water ring transportation pipeline. The pressure drop changes with time during the restart-up process are simulated and studied. With the aid of statistical product and service solutions (SPSS) software, regression analysis is performed on the four-factor mixed horizontal orthogonal restart experiment data to establish a multivariate nonlinear maximum restart pressure drop prediction model. By the analysis of the characteristics of each stage of the restart-up process, an exponential decay model of the restart pressure drop with time is set up. The research results can provide theoretical support and practical guidance for formulating appropriate restart-up plans for on-site shutdown pipelines, effectively avoiding safety risks.

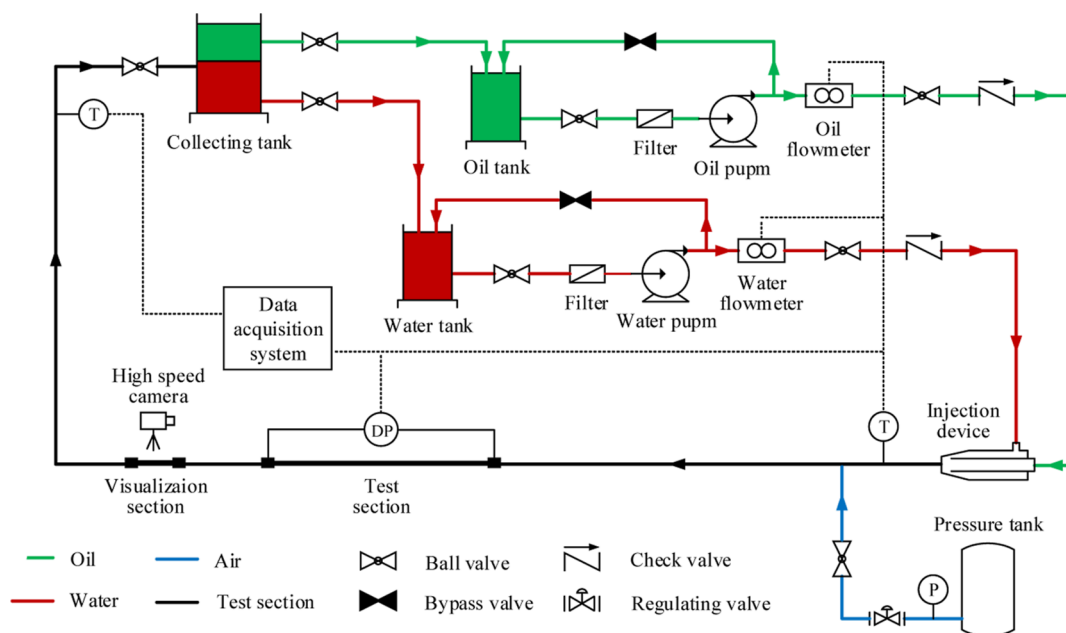
2. MATERIALS AND METHODS

2.1. Materials. The working fluids utilized for this experimental study are four representative types of ordinary heavy oil, collected from the Lvda oilfield within the Chinese Bohai Sea district, and tap water (pH 7.32 and salinity 132 mg/L) was used as the fluid of lubrication instead of the oilfield-produced water. For convenience of expression, the four viscous oil samples are recorded as LD1, LD2, LD3, and LD4, respectively. HAAKE Viscotester iQ Air rheometer (Karlsruhe, Germany) was adopted to test the viscosity properties of LD1–LD4 including rheological characteristics (see Figure 1a–d) and viscosity–temperature characteristics (see Figure 1e). It can be seen that all of the oil samples display a Newtonian fluid behavior within the temperature range of 20–70 °C, and each of their viscosities shows a trend of first decreasing sharply and then tending to stabilize with increasing temperature. A capillary stoppered pycnometer (Zhengzhou, China) was applied to determine the densities of the working fluids. A JJ2000B spinning drop interface tensiometer (Shanghai, China) that has a broad measurement range of 10^{-5} – 10^2 mN/m was employed to measure the interface tensions between LD1–LD4 and tap water. Table 1 lists the basic physical properties of these fluids.

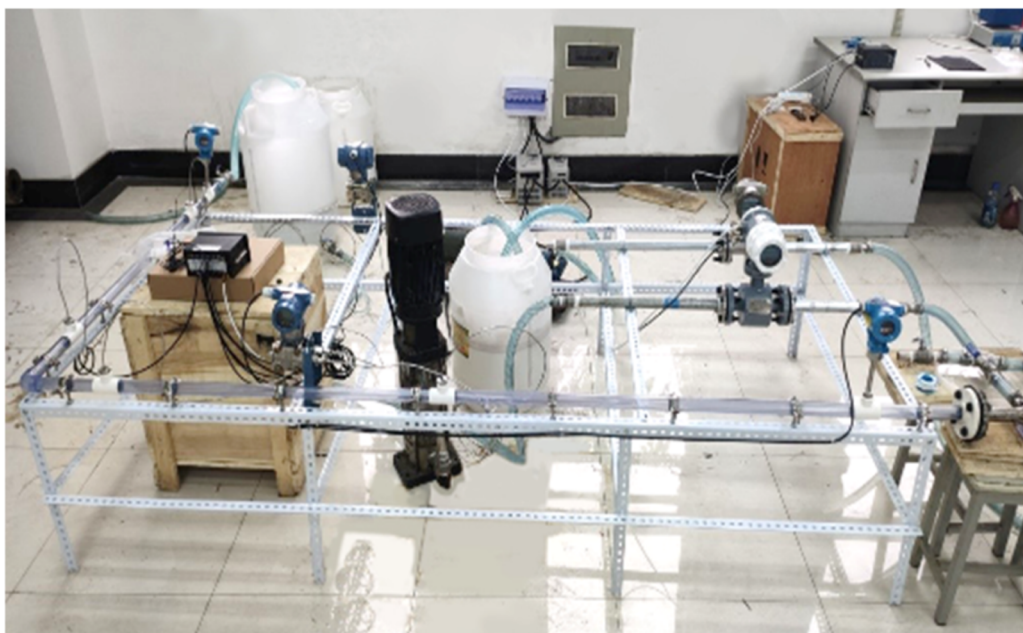
2.2. Experimental Facility. The multiphase flow loop used to conduct the flow, shutdown, and restart-up experiments of heavy oil–water core-annular flow (CAF) is shown in Figure 2. The facility primarily composes of five parts: liquid storage and

Table 1. Basic Physical Properties of the Working Fluids at 20 °C

physical parameters	Lvda heavy oil				tap water
	LD1	LD2	LD3	LD4	
density (kg/m ³)	902.0	912.6	920.1	928.4	998.2
viscosity (Pa·s)	1.0553	2.038	2.55	3.02	0.001
interfacial tension (mN/m)	34.6	34.83	33.53	32.26	



(a) The flow diagram of the experimental facility



(b) The actual picture of the experimental facility

Figure 2. Schematic of the experimental facility.

supply system, pipeline testing system, separation system, purge system, and data acquisition system. The test pipeline is made of unplasticized polyvinyl chloride (UPVC) with an internal diameter of 25 mm and a total length of 10 m. The choice of UPVC is based upon two considerations. One is that the flow resistance characteristics of heavy oil can be approximately simulated since the UPVC pipe has similar lipophilicity to steel pipes frequently used in field; the other is that the flow behaviors can be observed easily because of the inherent transparency of UPVC material. The injection device²⁸ located at the entrance of the test section, consisting of two concentric cylinders with a gap of 2 mm, is specifically designed to promote the formation of a CAF.

The heavy oil stored in a 50 L tank was delivered by a ZYB-83.3 residual oil pump (Hebei, China) to the center of the injection device. In the meantime, tap water was drawn from a tank with a capacity of 50 L and pumped into the annulus of the injection device by a CVL4-16 centrifugal pump (Guangdong, China). Before entering the injection device, the flow rate of oil was measured by a LWGY-830 turbine flowmeter (Tianjin, China) with a maximum measuring capacity of 10 m³/h and measurement accuracy of 0.5%, while that of water was metered by a LDC-QX315 electromagnetic flowmeter (Tianjin, China) with a measurement capacity of up to 7 m³/h and 0.5% measuring uncertainty. The injected flow rates of both fluids were individually adjusted and controlled through the frequency



Figure 3. Examples of heavy oil–water CAF.

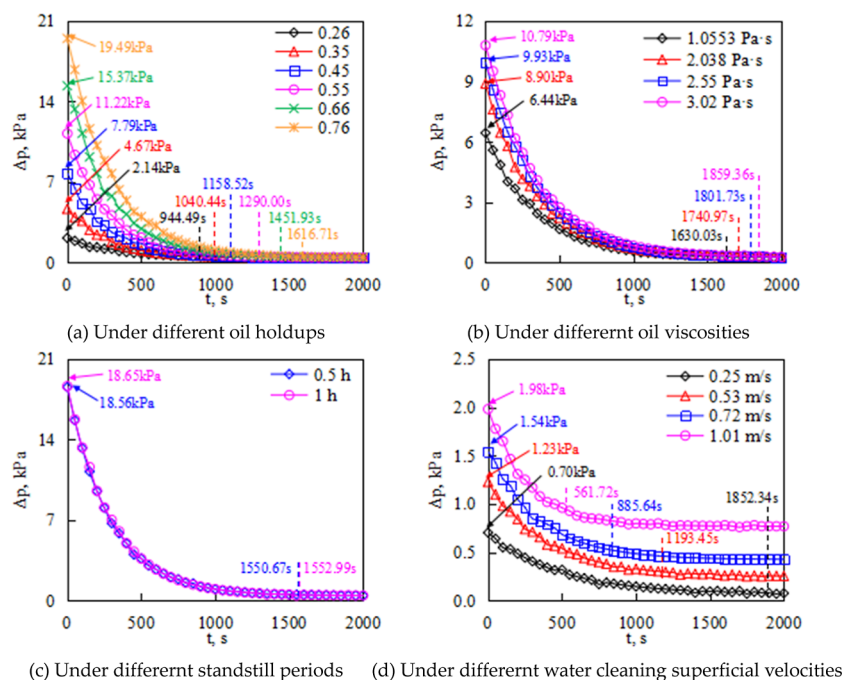


Figure 4. Variation curve of the restart-up pressure drop with time under different test conditions.

converter or bypass valve of the pump. After the oil and water flow through the test section, the mixture of them was discharged into a collecting tank with a capacity of 100 L, where it is separated under the action of gravity. Ultimately, the two fluids return to their individual storage tanks before they can be recirculated.

During the restart-up process, pressure drop was measured by a CYQ-3051DP differential pressure transducer (Tianjin, China), whose two ports are positioned at 5.5 and 7 m downstream from the injection device, respectively. The measurement range of this differential pressure transducer was 0–50 kPa and the accuracy was below 0.1%. Also, the fluid temperatures at the inlet and outlet of the test line were determined by CWQ-316 temperature sensors (Tianjin, China). A data acquisition system connected to a computer allows the monitoring, collection, and storage of flow rate, temperature, and pressure drop signals obtained from the online instruments in real time. All of the images were recorded using a Revealer2F04C high-speed camera (Hefei, China) with the aid of LED flood light through the visualization section.

2.3. Experimental Procedures. All the experiments were carried out in the horizontal configuration at 20 °C. Before performing the shutdown and restart-up experiments, it is necessary to first establish a stable CAF. Therefore, according to the criteria of stable CAF proposed by Bannwart,²⁹ the oil superficial velocity U_{os} was set to a fixed value of 0.74 m/s and the water superficial velocity U_{ws} was set in a range of 0.17–1.43 m/s. The outline of the experimental procedure is as follows. First, a CAF configuration was produced by injecting the heavy oil and water into the pipe through the injection device. The

examples of heavy oil–water CAF for different superficial velocity combinations are displayed in Figure 3. Second, both pumps were suddenly turned off to simulate a pump failure, and at the same time, all the valves were closed to trap oil and water within the pipe. Then, there was a waiting period. Finally, the valves were opened, and then the water pump was turned on with water flowing alone in the pipe at the desired superficial velocity. It is worth noting that the pipe needs to be cleaned up before each run; otherwise, the oil fouling adhering to the pipe surface will affect the measurement accuracy of the pressure drop. After all the experiments under different parameter conditions were completed, the testing system was flushed with water first and then blown with air.

3. RESULTS AND DISCUSSIONS

3.1. Evolution Characteristics of Pressure Drop in the Process of the Restart-Up. The relationship between pressure drop and time during the restart under different test conditions is presented in Figure 4. It can be seen that the four factors of oil holdup, oil viscosity, standstill period, and water cleaning superficial velocity all have an effect on the restart pressure drop and restart time. In Figure 4a, under the conditions of an oil viscosity μ_o of 2.038 Pa·s, a standstill period t_{st} of 1.0 h, and a water cleaning superficial velocity U_{cl} of 0.72 m/s, the maximum restart pressure drops Δp_{max} for different oil holdups H_o of 0.26, 0.35, 0.45, 0.55, 0.66, and 0.76 are 2.14, 4.67, 7.79, 11.22, 15.37, and 19.49 kPa, and the restart times t_r are 944.49, 1040.44, 1158.52, 1290.00, 1451.93, and 1616.71 s. As shown in Figure 4b, in the circumstances of H_o of 0.55, t_{st} of 0.5 h, and U_{cl} of 0.53 m/s, the Δp_{max} are 6.44, 8.90, 9.93, and 10.79 kPa at various μ_o of

1.0553, 2.038, 2.55, and 3.02 Pa·s. The corresponding restart times t_r are 1630.03, 1740.97, 1801.73, and 1859.36 s, respectively. In Figure 4c, at the conditions of H_o of 0.66, μ_o of 3.02 Pa·s, and U_{cl} of 0.72 m/s, the Δp_{max} values for different t_{st} of 0.5 and 1.0 h are 18.56 and 18.65 kPa, and the restart times are 1550.67 and 1552.99 s. As displayed in Figure 4d, in the cases of H_o of 0.26, μ_o of 1.0553 Pa·s, and t_{st} of 0.5 h, the Δp_{max} values are 0.70, 1.23, 1.54, and 1.98 kPa for various U_{cl} of 0.25, 0.53, 0.72, and 1.01 m/s. The corresponding restart times t_r are 1852.34, 1193.45, 885.64, and 561.72 s, respectively. With these examples, it can be inferred that the oil holdup, oil viscosity, and water cleaning superficial velocity have a great influence on the restart characteristics, while the standstill period has a minimal impact on the restart characteristics.

Moreover, a comparison of Figure 4a–d indicates that the evolution characteristics of the restart pressure drop over time under different operating conditions have similarity. That is, as time passes by, the pressure drop first rapidly decreases from the initial peak value and then slowly decreases until it approaches a value near the steady-state pressure drop of single-phase water flow. This result is consistent with the previous findings of Poesio and Strazza³⁰ and Livinus et al.,³¹ but there are differences in the shape of the pressure drop evolution along with time, especially in the falling stage. Further analysis reveals that the restart-up process can be generally divided into two stages, including the decay stage and steady stage (see Figure 5).

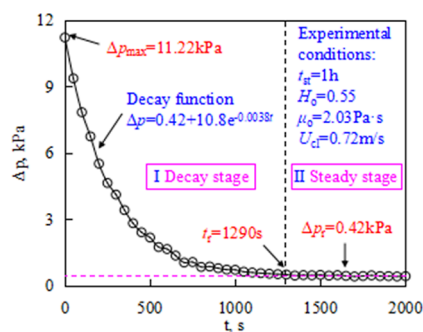


Figure 5. Change law of restart-up pressure drop with time.

In the decay stage (stage I), the pressure drop shows the trend of dropping dramatically at first and then gradually slowing down against time. This is because, in the beginning period, the water flow quickly pushes a large amount of viscous oil out of the pipe (Figure 6a), followed by gradual clearance of the adhered oil film on the pipe inner wall (Figure 6b). In the steady stage (stage II), the restart pressure drop remains basically unchanged or exhibits a slight fluctuation around a certain constant value with the increase in time. This is because almost all of the viscous oil has been removed from the pipe by the water flow, and there is only water flowing in the pipe (see Figure 6c).



Figure 6. Evolution of heavy oil–water flow regimes during the restart-up process.

By fitting the experimental data of the restart pressure drop, it can be found that the pressure drop variation with time during the restart-up process can be well described by the function relationship shown in eq 1. As can be seen from eq 1, in the decay stage, the restart pressure drop is an exponential decline curve along time, while in the steady stage, the restart pressure drop is independent of time and its value is equal to the steady-state pressure drop value of single-phase water flow.

$$\begin{cases} \Delta p = \Delta p_r + (\Delta p_{max} - \Delta p_r)e^{-Bt} & (0 \leq t < t_r) \\ \Delta p \approx \Delta p_r & (t \geq t_r) \end{cases} \quad (1)$$

3.2. Nonlinear Regression Model of Maximum Restart Pressure Drop. Based on the analysis of the pressure drop variation and its characteristics during the restart-up process, it can be concluded that the maximum pressure drop is a necessary and key parameter for accurately describing the relationship between the pressure drop and time during the restart-up process. A quantitative correlation between the maximum pressure drop and its influencing factors, including oil holdup, standstill period, oil viscosity, and superficial water cleaning velocity, must be established. Therefore, an orthogonal experiment with four factors and a mixed level is conducted. The factors and levels of the orthogonal restart-up experiment for heavy oil–water ring transportation pipeline are listed in Table 2.

Table 2. Factors and Levels of the Orthogonal Restart-Up Experiment for Heavy Oil–Water Ring Transportation Pipeline

level	H_o	μ_o (Pa·s)	t_{st} (h)	U_{cl} (m/s)
1	0.26	1.0553	0.5	0.25
2	0.35	2.038	1.0	0.53
3	0.45	2.55		0.72
4	0.55	3.02		1.01
5	0.66			
6	0.76			

Guided by the principle of orthogonal experiment design, a restart-up experiment scheme $L_{32} (6^1 \times 2^1 \times 4^2)$ is put forward. Table 3 shows the scheme and results of the orthogonal experiment. For the purpose of exploring the influencing extent of each factor on the maximum restart pressure drop and building the model of the maximum restart pressure drop, the SPSS software is applied to perform variance and regression analysis on the results of the orthogonal experiment.

The analysis of variance of orthogonal experiment results is illustrated in Table 4. Through comparison of F -value of various factors, we know that the oil holdup and water cleaning superficial velocity are the greatest, oil viscosity is medium, and standstill period contributes minor to the four factors affecting the maximum restart pressure drop. In other words, oil holdup

Table 3. Scheme and Results of the Orthogonal Experiment

test	H_o	μ_o (Pa·s)	t_{st} (h)	U_{cl} (m/s)	Δp_{max} (kPa)
1	3	2	2	1	3.413
2	2	1	1	3	3.216
3	1	4	2	4	3.418
4	1	2	1	3	1.782
5	4	1	1	4	10.934
6	2	1	2	2	2.885
7	1	1	2	4	1.345
8	5	4	1	2	14.026
9	2	4	1	3	4.687
10	2	3	2	4	6.602
11	2	3	1	1	2.215
12	1	3	2	2	2.295
13	1	2	2	2	1.964
14	4	3	1	2	9.715
15	5	1	2	3	11.024
16	2	2	2	4	5.872
17	3	4	2	3	10.336
18	5	3	2	1	8.824
19	6	3	2	3	20.378
20	3	3	1	4	11.120
21	2	4	2	2	4.689
22	5	2	1	4	18.764
23	1	3	1	3	2.103
24	2	2	1	1	2.058
25	6	1	2	1	6.125
26	6	2	1	2	15.680
27	4	2	2	3	11.096
28	1	1	1	1	0.790
29	4	4	2	1	6.002
30	6	4	1	4	29.985
31	3	1	1	2	4.903
32	1	4	1	1	1.198

Table 4. Analysis of Variance of the Orthogonal Experiment Results

	H_o	μ_o (Pa·s)	t_{st} (h)	U_{cl} (m/s)
F value	26.853	3.393	3.237	10.046
sig. value	0.000	0.039	0.088	0.000

and water cleaning superficial velocity are the primary factors, while oil viscosity and the standstill period are the secondary factors. The influence degree of the four factors on maximum restart pressure drop is ranked from high to low as oil holdup, water cleaning superficial velocity, oil viscosity, and standstill period.

Given that the four factors that affect the maximum pressure drop have different ranges of values and units of measurement, in order to eliminate the differences in order of magnitude and dimension among these factors and reduce the fitting error of the nonlinear regression model, the minimum–maximum value-based normalization method³² is applied to normalize the original data. This method performs a linear transformation on the original data, converting it into a dimensionless index evaluation value and mapping the data values to the range of 0–1. The conversion formula is given in eq 2.

$$\tilde{x} = \frac{x - x_{\min}}{x_{\max} - x_{\min}} \quad (2)$$

In accordance with the range of each influencing factor (Table 2), the conversion formula for each factor can be obtained using eq 2, as shown in eq 3.

$$\tilde{H}_o = \frac{H_o - 0.26}{0.76 - 0.26}, \tilde{\mu}_o = \frac{\mu_o - 1.0553}{3.02 - 1.0553}, \tilde{t}_{st} = \frac{t_{st} - 0.5}{1 - 0.5}, \tilde{U}_{cl} = \frac{U_{cl} - 0.25}{1.01 - 0.25} \quad (3)$$

The results of the orthogonal experiment are normalized and combined with the analysis of the effect of various factors on the maximum restart pressure drop, a multivariate nonlinear regression model is set up to predict the maximum restart pressure drop; see eq 4.

$$\Delta p_{\max} = a \cdot (b + cH_o + dH_o^2) \cdot \mu_o^e \cdot t_{st}^f \cdot U_{cl}^g \quad (4)$$

The SPSS software is used to fit the nonlinear regression model and test its correlation coefficient. Due to the maximum relative reduction between the sum of squares of continuous residuals being 1.000×10^{-8} ,³³ the system stopped running after 49 model evaluations and 21 derivative evaluations. The resulting nonlinear regression model has a determination coefficient R^2 of 0.995, which is very close to 1, indicating that the model has an accurate goodness of fit. Therefore, the optimal estimated values of the nonlinear regression coefficients can be obtained through iterative calculations. Substituting the specific values of each coefficient into eq 4, a multivariate nonlinear regression model for the maximum pressure drop during restart-up of the heavy oil–water-lubricated transportation pipeline can be obtained; see eq 5.

$$\Delta p_{\max} = 23.820 \cdot (-170.644 + 836.686H_o + 436.568H_o^2) \cdot \mu_o^{0.480} \cdot t_{st}^{0.006} \cdot U_{cl}^{0.726} \quad (5)$$

According to the analysis of eq 5, it can be concluded that the maximum restart pressure drop increases correspondingly with the increase of oil holdup, showing a quadratic function trend. Moreover, as the oil holdup increases, the growth rate of the maximum restart pressure decrease becomes more and more obvious. The maximum restart pressure drop exponentially increases with the oil viscosity, standstill period, and water cleaning superficial velocity; that is, with the increase of oil viscosity, standstill period, and water cleaning superficial velocity, the maximum restart pressure drop increases. However, the larger the oil viscosity, standstill period, and water cleaning superficial velocity, the slower the growth rate of the maximum restart pressure drop.

3.3. Model of Restart Pressure Drop Variation with Time. In the model of restart pressure drop changing with time (see eq 1), maximum restart pressure drop can be calculated based on the multivariate nonlinear regression model (see eq 5), and the stable pressure drop, which is equal to the steady-state pressure drop of single-phase water flow, can be calculated according to Darcy-Weisbach formula.³⁴ Therefore, eq 1 can be embodied as eq 6.

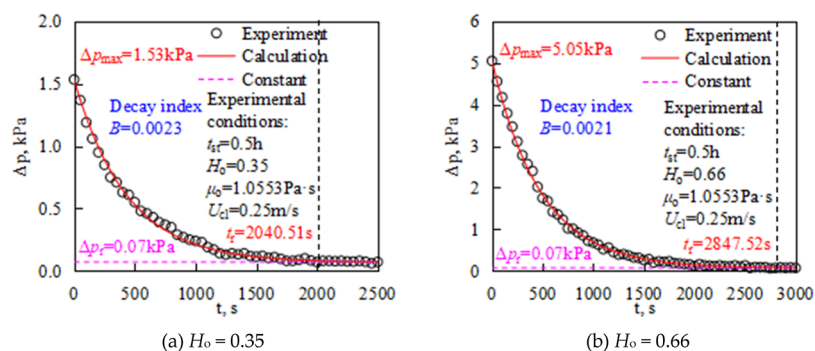


Figure 7. Comparison between experimental value and fitted value of restart-up pressure drop under different oil holdups.

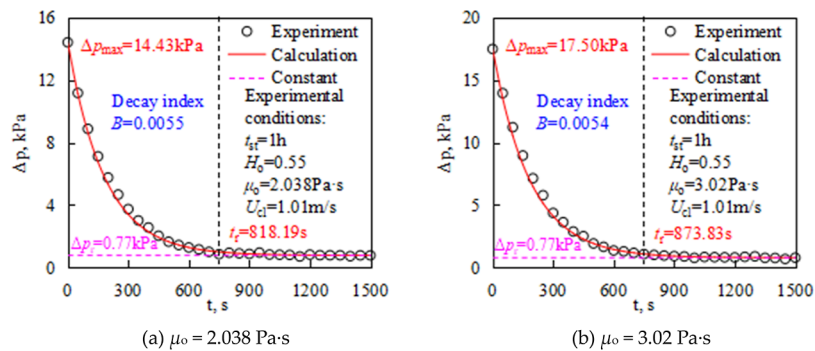


Figure 8. Comparison between experimental value and fitted value of restart-up pressure drop under different oil viscosities.

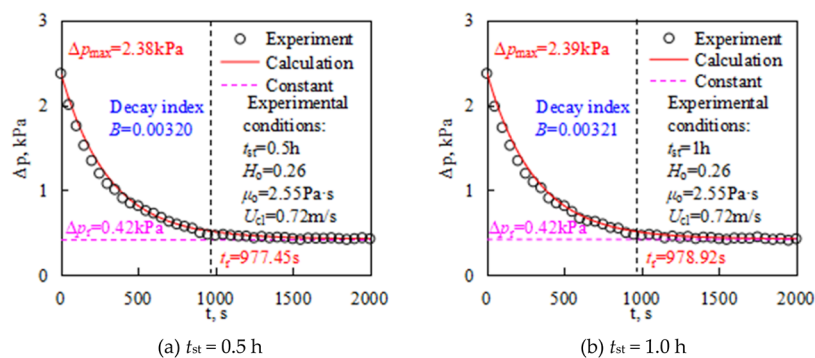


Figure 9. Comparison between experimental value and fitted value of restart-up pressure drop under different standstill periods.

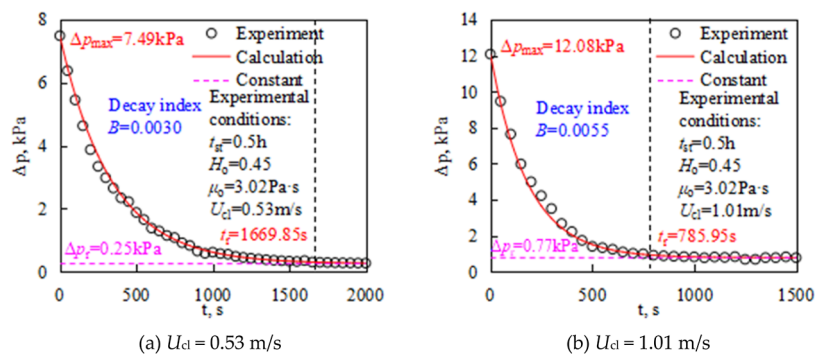


Figure 10. Comparison between experimental value and fitted value of restart-up pressure drop under different water cleaning superficial velocities.

$$\left\{ \begin{array}{l} \Delta p = \lambda \frac{L \rho_w U_{cl}^2}{D} + 23.820 \cdot \\ \quad (-170.644 + 836.686H_o \\ \quad + 436.568H_o^2) \cdot \mu_o^{0.480} \cdot t_{st}^{-0.006} \cdot U_{cl}^{0.726} \cdot \\ \quad e^{-Bt} - \lambda \frac{L \rho_w U_{cl}^2}{D} \cdot e^{-Bt} \\ \Delta p \approx \lambda \frac{L \rho_w U_{cl}^2}{D} \end{array} \right. \quad \begin{array}{l} (0 \leq t < t_r) \\ \\ \\ (t \geq t_r) \end{array} \quad (6)$$

In order to explore the behavior characteristics of the restart-up process of the heavy oil–water-lubricated transportation pipeline and compare the fitting results of the restart pressure drop model with the experimental data, the typical working conditions under different oil holdups, oil viscosities, standstill periods, and water cleaning superficial velocities are analyzed and explained. The comparison results of the experimental measured values and model fitting values of restart pressure drop under four typical working conditions are shown in Figures 7–10, respectively. It can be seen from the figure that under different test conditions, the behavior characteristics of the restart-up process of the heavy oil–water-lubricated transportation pipeline are similar; that is, the restart pressure drop in the initial stage decreases sharply from the maximum value, then decreases slowly, and finally no longer changes with time. Taking Figure 7b as an example, the restart pressure drop rapidly drops from the maximum value of 5.05 kPa at the initial time of 0 s to 1.01 kPa (20% of the maximum value), which is completed in a relatively short time of 800 s. Subsequently, the restart pressure slowly decreases from 1.01 to 0.07 kPa within a longer period of 2047.52 s. Finally, when the running time exceeds 2847.52 s, the restart pressure drop keeps a small fluctuation near 0.07 kPa. However, the specific values of the two key parameters that describe the behavior characteristics of the restart-up process, namely, the maximum restart pressure drop and the restart time, are different. Taking Figure 8a,b for instance, under the conditions of an oil holdup of 0.55, a standstill period of 1.0 h, and a water cleaning superficial velocity of 1.01 m/s, when the oil viscosity is 2.038 Pa·s, the maximum restart pressure drop is 14.43 kPa, and the corresponding restart time is 818.19 s, while when the oil viscosity is 3.02 Pa·s, the maximum restart pressure drop is 17.50 kPa, and the corresponding restart time is 873.83 s.

Through the contrastive analysis of parts a,b in Figures 7–10, it can be observed that the restart time increases with the increase of oil holdup and oil viscosity, basically unchanged with the increase of standstill period, but decreases with the increase of water cleaning superficial velocity. This is consistent with the change rule of restart time with various influencing factors obtained by Strazza and Poesio.³⁵ In addition, it can be seen from the figure that the length of the restart time can be reflected by the decay index B , where the larger the decay index, the shorter the restart time. Taking Figure 10a,b as examples, in the circumstances of an oil holdup of 0.45, a standstill period of 0.5 h, and an oil viscosity of 3.02 Pa·s, when the water cleaning superficial velocity is 0.53 and 1.01 m/s, the decay index is 0.0030 and 0.0055 1/s, and the corresponding restart time is 1669.85 and 785.95 s. In practical engineering, measures such as increasing the water cleaning superficial velocity or restarting flow can be taken to shorten the restart time required for the shutdown pipelines. However, attention should also be paid to whether the increase in the maximum restart pressure drop

caused by the increase in the water flow rate is within the allowable range of the pressure drop of the pipeline system. Zagustin et al.³⁶ proposed a method of gradually increasing the water flow velocity to solve the problem of excessive maximum pressure drop during restart-up due to the increase in water flow velocity. This method can not only ensure that the maximum restart pressure drop is not too high but also shorten the restart time. However, it is worth noting that this method is applicable only to lipophilic and hydrophobic pipelines. For hydrophilic and oleophobic pipelines, it is more effective to directly restart the pipeline with a higher water flow velocity.³⁵ In addition, the goodness of fit R^2 of restart pressure drop for four typical working conditions are 0.979 (Figure 7a), 0.988 (Figure 7b), 0.983 (Figure 8a), 0.985 (Figure 8b), 0.962 (Figure 9a), 0.958 (Figure 9b), 0.976 (Figure 10a), and 0.981 (Figure 10b), all of which are very close to 1, indicating that the model fitting values of pressure drop changes during restart are in good agreement with the experimental measurements.

4. CONCLUSIONS

In the present work, an experimental survey is executed to explore the restart characteristics of a heavy oil–water ring transportation pipeline from a stratified configuration under varying operating conditions. Also, the four-factor mixed horizontal orthogonal experimental results have been used to formulate correlations for the prediction of the restart-up process.

- (1) During the restart-up process of heavy oil–water ring transportation pipeline with a constant water flow velocity, the restart pressure drop varies along with time, showing a trend of rapid declining at first, then slowing down until reaching a constant value. This process can be generally divided into two stages: decay stage and steady stage.
- (2) Based on the four-factor mixed level orthogonal restart experiment, the variance and regression analysis of 32 groups of orthogonal experiment results are carried out by adopting the SPSS software, and a multivariate nonlinear regression prediction model of maximum restart pressure drop is established.
- (3) In light of the behavior characteristics of restart-up process of heavy oil–water ring transportation pipeline, an exponential model of restart pressure drop with time is established. The model fitting values of pressure drop changes during restart are highly consistent with the experimental measurement values, and their goodness of fit are all very close to 1.
- (4) The increase in oil holdup, oil viscosity, and standstill period will not only increase the maximum restart pressure drop but also increase the restart time; the increase in water cleaning superficial velocity can shorten the restart time but will increase the maximum pressure drop. Therefore, for a given oil–water throughput and heavy oil type, the restart-up of the shutdown pipeline can be improved by shortening the standstill period as much as possible during the shutdown and appropriately increasing the water cleaning superficial velocity during the restart-up.

AUTHOR INFORMATION

Corresponding Authors

Xiaoyun Yin – Safety, Environment and Technology Supervision Research Institute of PetroChina Southwest Oil and Gas Field Company, Chengdu 610041, China; Shale Gas Evaluation and Exploitation Key Laboratory of Sichuan Province, Chengdu 610041, China; orcid.org/0000-0001-6970-1348; Email: yinxy0122@163.com

Jiaqiang Jing – School of Oil & Natural Gas Engineering, Southwest Petroleum University, Chengdu 610500, China; Oil & Gas Fire Protection Key Laboratory of Sichuan Province, Chengdu 611731, China; orcid.org/0000-0003-4219-0829; Email: jjq@swpu.edu.cn

Authors

Ming Wen – Safety, Environment and Technology Supervision Research Institute of PetroChina Southwest Oil and Gas Field Company, Chengdu 610041, China; Shale Gas Evaluation and Exploitation Key Laboratory of Sichuan Province, Chengdu 610041, China

Dong Lin – Safety, Environment and Technology Supervision Research Institute of PetroChina Southwest Oil and Gas Field Company, Chengdu 610041, China; Shale Gas Evaluation and Exploitation Key Laboratory of Sichuan Province, Chengdu 610041, China

Jiayi Li – Pipeline Co. Ltd. of Guizhou Province, PetroChina Southwest Pipeline Co. Ltd., Chengdu 610000, China

Zhen Zhu – PetroChina Southwest Oil and Gas Field Company, Chengdu 610051, China

Yu Zhang – PetroChina Southwest Oil and Gas Field Company, Chengdu 610051, China

Jinyan Hu – Safety, Environment and Technology Supervision Research Institute of PetroChina Southwest Oil and Gas Field Company, Chengdu 610041, China; Shale Gas Evaluation and Exploitation Key Laboratory of Sichuan Province, Chengdu 610041, China

Pengsheng Zeng – Safety, Environment and Technology Supervision Research Institute of PetroChina Southwest Oil and Gas Field Company, Chengdu 610041, China; Shale Gas Evaluation and Exploitation Key Laboratory of Sichuan Province, Chengdu 610041, China

Jie Sun – School of Oil & Natural Gas Engineering, Southwest Petroleum University, Chengdu 610500, China; Oil & Gas Fire Protection Key Laboratory of Sichuan Province, Chengdu 611731, China

Complete contact information is available at:

<https://pubs.acs.org/10.1021/acsomega.4c00185>

Author Contributions

All authors made substantial contributions to the manuscript. The manuscript to be submitted was approved by all the authors. The authors did the following work: methodology, investigation, data curation, and original draft preparation, X.Y.; investigation, methodology, and supervision, M.W.; investigation, validation, and review and editing, D.L. and J.L.; review and editing, Z.Z. and Y.Z.; formal analysis and resources, J.H. and P.Z.; formal analysis and validation, J.J. and J.S. All authors have read and agreed to the published version of the manuscript.

Notes

The authors declare no competing financial interest.

ACKNOWLEDGMENTS

This program was sponsored by the National Natural Science Foundation of China (nos. U19B2012 and 52106208) and the Natural Science Foundation of Sichuan Province (no. 2023NSFSC0924).

NOMENCLATURE

a	viscous modulus, Pa
B	decay index, 1/s
b	regression coefficient
c	regression coefficient
D	pipe diameter, m
d	regression coefficient
e	regression coefficient
f	regression coefficient
g	regression coefficient
H_o	oil holdup
\tilde{H}_o	normalized oil holdup
L	pipe length, m
Δp	restart pressure drop, Pa
Δp_{\max}	maximum restart pressure drop, Pa
Δp_r	stable pressure drop, Pa
t	running time of restart-up process, s
t_{st}	standstill period, h
\tilde{t}_{st}	normalized standstill period, h
t_r	restart time, s
U_{cl}	water cleaning superficial velocity, m/s
\tilde{U}_{cl}	normalized water cleaning superficial velocity, m/s
U_{os}	oil superficial velocity, m/s
U_{ws}	water superficial velocity, m/s
x	actual value of the original data
x_{\min}	minimum value of the original data
x_{\max}	maximum value of the original data
\tilde{x}	normalized value of the original data

GREEK LETTERS

λ	hydraulic friction coefficient
μ_o	oil viscosity, Pa·s
$\tilde{\mu}_o$	normalized oil viscosity, Pa·s
ρ_w	water density, kg/m ³

SUBSCRIPTS

o	oil phase
w	water phase

ABBREVIATIONS

SPSS	statistical product and service solutions
CAF	core-annular flow
UPVC	unplasticized polyvinyl chloride
ID	internal diameter

REFERENCES

- Jing, J.; Yin, X.; Mastobaev, B. N.; Vavar, A. R.; Sun, J.; Wang, S.; Liu, H.; Zhuang, L.; Fan, Z. Drag reduction characteristics of water annulus transportation of simulated heavy oil in horizontal pipeline. *Chem. Eng. Res. Des.* **2021**, *40* (2), 635–641.
- Sun, J.; Guo, L.; Yin, X.; Jing, J.; Fu, J.; Lu, Y.; Ullmann, A.; Brauner, N. Investigation on drag reduction of aqueous foam for transporting thermally produced high viscosity oil. *J. Pet. Sci. Eng.* **2022**, *210*, 110062.
- Sun, J.; Guo, L.; Fu, J.; Jing, J.; Yin, X.; Lu, Y.; Ullmann, A.; Brauner, N. A new model for viscous oil-water eccentric core annular flow in horizontal pipes. *Int. J. Multiphase Flow* **2022**, *147*, 103892.

- (4) Lyu, Y.; Huang, Q. Y. Flow characteristics of heavy oil-water flow during high water-content cold transportation. *Energy* **2023**, *262*, 125441.
- (5) Kumar Sharma, V.; Singh, A.; Tiwari, P. An experimental study of pore-scale flow dynamics and heavy oil recovery using low saline water and chemical flooding. *Fuel* **2023**, *334*, 126756.
- (6) Yin, X.; Li, J.; Wen, M.; Dong, X. J.; You, X.; Su, M.; Zeng, P.; Jing, J.; Sun, J. Study on the Hydrodynamic Performance and Stability Characteristics of Oil-Water Annular Flow through a 90° Elbow Pipe. *Sustainability* **2023**, *15*, 6785.
- (7) dos Santos, L. A.; Ribeiro, D. da C.; Romero, O. J. Heavy oil transportation through steam heating: An analytical and numerical approach. *J. Pet. Sci. Eng.* **2020**, *195*, 107932.
- (8) Zaman, M.; Bjorndalen, N.; Islam, M. R. Detection of precipitation in pipelines. *Pet. Sci. Technol.* **2004**, *22* (9–10), 1119–1141.
- (9) Ashrafzadeh, S. N.; Kamran, M. Emulsification of heavy crude oil in water for pipeline transportation. *J. Pet. Sci. Eng.* **2010**, *71* (3–4), 205–211.
- (10) Milligan, S. N.; Johnston, R. L.; Burden, T. L.; Burden, T. L.; Dreher, W. R.; Smith, K. W. Drag reduction of asphaltic crude oils. U.S. Patent. 8,022,118 B2, 2013, 8450251. <https://patents.google.com/patent/US8022118B2>.
- (11) Ghosh, S.; Mandal, T. K.; Das, G.; Das, P. K. Review of oil water core annular flow. *Renewable Sustainable Energy Rev.* **2009**, *13* (8), 1957–1965.
- (12) Al-Muntaser, A. A.; Varfolomeev, M. A.; Suwaid, M. A.; Saleh, M. M.; Djimasbe, R.; Yuan, C. D.; Zairov, R. R.; Ancheyta, J. Effect of decalin as hydrogen-donor for in-situ upgrading of heavy crude oil in presence of nickel-based catalyst. *Fuel* **2022**, *313*, 122652.
- (13) Hart, A. A review of technologies for transporting heavy crude oil and bitumen via pipelines. *J. Pet. Explor. Prod. Technol.* **2014**, *4*, 327–336.
- (14) Bensakhria, A.; Peysson, Y.; Antonini, G. Experimental Study of the Pipeline Lubrication for Heavy Oil Transport. *Oil Gas Sci. Technol.* **2004**, *59* (5), 523–533.
- (15) Wu, J.; Jiang, W.; Du, S.; Liu, Y. Experiment on drag reduction of heavy oil in horizontal pipeline by water annular conveying. *CIESC J.* **2019**, *70* (5), 1734–1741.
- (16) Jiang, W. M.; Du, S. L.; Wu, J. Q.; Liu, Y.; Bian, J. Structural optimization of core-annular flow generator for the heavy oil transportation. *Oil Gas Storage Transp.* **2019**, *38* (8), 937–943.
- (17) Yin, X.; Fu, L.; Li, J.; Cheng, S.; Jing, J.; Mastobaev, B. N.; Sun, J. Analysis of restart-up pressure drop characteristics of heavy oil-water ring transportation pipeline. *Chem. Eng. Res. Des.* **2023**, *42* (11), 5669–5679.
- (18) Ooms, G.; Vuik, C.; Poesio, P. Core-annular flow through a horizontal pipe: Hydrodynamic counterbalancing of buoyancy force on core. *Phys. Fluids* **2007**, *19* (9), 092103.
- (19) Ooms, G.; Pourquie, M. J. B. M.; Beerens, J. C. On the levitation force in horizontal core-annular flow with a large viscosity ratio and small density ratio. *Phys. Fluids* **2013**, *25* (3), 032102.
- (20) Jing, J.; Yin, X.; Mastobaev, B. N.; Valeev, A. R.; Sun, J.; Wang, S.; Liu, H.; Zhuang, L. Experimental study on highly viscous oil-water annular flow in a horizontal pipe with 90° elbow. *Int. J. Multiphase Flow* **2021**, *135*, 103499.
- (21) Strazza, D.; Grassi, B.; Demori, M.; Ferrari, V.; Poesio, P. Core-annular flow in horizontal and slightly inclined pipes: Existence, pressure drops, and hold-up. *Chem. Eng. Sci.* **2011**, *66* (12), 2853–2863.
- (22) Ingen Housz, E. M. R. M.; Ooms, G.; Henkes, R. A. W. M.; Pourquie, M. J. B. M.; Kidess, A.; Radhakrishnan, R. A comparison between numerical predictions and experimental results for horizontal core-annular flow with a turbulent annulus. *Int. J. Multiphase Flow* **2017**, *95*, 271–282.
- (23) Shi, J.; Al-Awadi, H.; Yeung, H. An experimental investigation of high-viscosity oil-water flow in a horizontal pipe. *Can. J. Chem. Eng.* **2017**, *95* (12), 2423–2434.
- (24) Hu, H. H.; Joseph, D. D. Lubricated pipelining: stability of core-annular flow. Part 2. *J. Fluid Mech.* **1989**, *205*, 359–396.
- (25) Chen, K.; Bai, R.; Joseph, D. D. Lubricated pipelining. Part 3 Stability of core-annular flow in vertical pipes. *J. Fluid Mech.* **1990**, *214*, 251–286.
- (26) Bannwart, A. C. Bubble analogy and stabilization of core-annular flow. *J. Energy Resour. Technol.* **2001**, *123* (2), 127–132.
- (27) Rodriguez, O. M. H.; Bannwart, A. C. Stability analysis of core-annular flow and neutral stability wave number. *AIChE J.* **2008**, *54* (1), 20–31.
- (28) Yin, X. Y.; Jing, J. Q.; Sun, J.; Liu, L. H.; Pu, B. Shutdown and restart characteristics on water ring transfer of heavy oil in horizontal pipeline. *China Pet. Mach.* **2022**, *50* (4), 124–129.
- (29) Bannwart, A. C. Modeling aspects of oil-water core-annular flows. *J. Pet. Sci. Eng.* **2001**, *32* (2–4), 127–143.
- (30) Poesio, P.; Strazza, D. Experiments on start-up of an oil-water core annular flow through a horizontal or nearly horizontal pipe. In *Proceedings of the 13th International Conference on Multiphase Production Technology, Edinburgh, UK, June, 13–15; OnePetro*, 2007, pp 79–87. <https://www.researchgate.net/publication/289779506>.
- (31) Livinus, A.; Yeung, H.; Lao, L. Restart time correlation for core annular flow in pipeline lubrication of high-viscous oil. *J. Pet. Explor. Prod. Technol.* **2017**, *7* (1), 293–302.
- (32) Maucec, M.; Jalali, R. GeoDIN - Geoscience-Based Deep Interaction Networks for Predicting Flow Dynamics in Reservoir Simulation Models. *SPE J.* **2022**, *27* (03), 1671–1689.
- (33) Wang, S.; Jing, J.; Song, X.; Shen, X.; Chen, L. Yield characteristics of heavy oil emulsion and prediction for pipeline start-up pressure. *Chem. Eng. Res. Des.* **2019**, *38* (9), 4020–4028.
- (34) Miller, F. P.; Vandome, A. F.; Mcbrewster, J. *Darcy-Weisbach Equation*; Alphascript Publishing: Saarbrücken, 1945.
- (35) Strazza, D.; Poesio, P. Experimental study on the restart of core-annular flow. *Chem. Eng. Res. Des.* **2012**, *90* (11), 1711–1718.
- (36) Zagustin, K.; Guevara, E.; Nunez, G. Process for restarting core flow with very viscous oils after a long standstill period. U.S. Patent 4,745,937 A, 1988. <https://www.freepatentsonline.com/4745937.html>.